

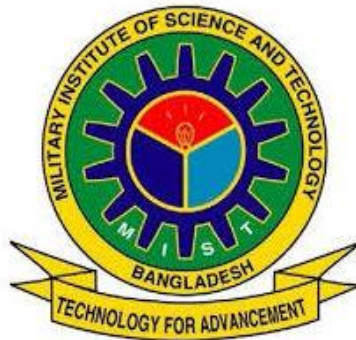
The Early Voltage and Current Gain of InGaAs Double Heterojunction Bipolar Transistor

A thesis submitted to the Department of Electrical, Electronics and Communication Engineering, Military Institute of Science and Technology, in partial fulfillment of the requirements for the degree of BACHELOR OF SCIENCE IN ELECTRICAL, ELECTRONICS AND COMMUNICATION ENGINEERING

Submitted by

MAJOR MUHAMMAD SANBIR HASAN MOJUMDER

JOAIRIA CHOWDHURY



Supervised by

YEASIR ARAFAT

Assistant Professor

**Department of Electrical and Electronic Engineering (EEE)
Bangladesh University of Engineering and Technology (BUET)**

Dhaka-1000, Bangladesh

December, 2013

The thesis titled “**The Early Voltage and Current Gain Of InGaAs Double Heterojunction Bipolar Transistor**” submitted by Major Muhammad Sanbir Hasan, Student No: 200816002, Joairia Chowdhury, Student No: 201016029, has been accepted as satisfactory in partial fulfillment of the requirements for the degree of BACHELOR OF SCIENCE IN ELECTRICAL, ELECTRONICS AND COMMUNICATION ENGINEERING on December, 2013.

APPROVAL OF THE SUPERVISOR

Yeasir Arafat

Assistant Professor

Department of Electrical and Electronic Engineering (EEE)
BUET, Dhaka-1000, Bangladesh.

DECLARATION

It is hereby declared that this thesis or any part of it has not been submitted elsewhere for the award of any degree or diploma.

Signatures of candidates

Major Muhammad Sanbir Hasan Mojumder
Student No:200816002

Joairia Chowdhury
Student No:201016029

DEDICATION

To Our Parents

TABLE OF CONTENTS

TITLE PAGE	i
CERTIFICATION	ii
DECLARATION	iii
LIST OF TABLES	viii
LIST OF FIGURES	ix
LIST OF ABBREVIATION	xiii
LIST OF TECHNICAL SYMBOLS AND TERMS	xv
ACKNOWLEDGEMENTS	xix
ABSTRACT	xx
CHAPTER 1: INTRODUCTION	1
1.1 THE TRANSISTOR	1
1.1.1 Brief history of transistor	1
1.1.2 Category of transistor	5
1.2 THE BIPOLAR TRANSISTOR	7
1.2.1 The dopants	8
1.2.2 The doping process of BJT	9
1.2.3 n^+ -p-n transistor operation	9
1.2.4 Advantages of bipolar transistor	12
1.3 HETEROJUNCTION BIPOLAR TRANSISTOR	12
1.3.1 The InGaAs device physics	15

1.3.2	The InGaAs HBT	19
1.3.3.	Applications of InGaAs HBT	21
CHAPTER 2:	BACKGROUND OF WORK	23
2.1	THE EARLY VOLTAGE AND COMMON EMITTER AND CURRENT GAIN	23
2.2	THE IMPORTANCE OF EARLY VOLTAGE AND CURRENT GAIN	27
2.3	REVIEW OF RECENT WORKS ON EARLY VOLTAGE AND CURRENT GAIN	27
2.4	SCOPE OF THE DISSERTATION	28
2.5	LAYOUT OF THE CHAPTERS	29
2.6	DERIVATION OF MAIN EQUATION	29
	2.4.1 Derivation of collector current density, J_{CO}	30
	2.4.2 Early voltage	31
	2.4.3 Electric field	32
2.7	CONCLUSION	33
CHAPTER 3:	MATHEMATICAL ANALYSIS	34
3.1	INTRODUCTION	34
3.2	DERIVATION OF THE MODEL EQUATIONS	35
	3.2.1 Low injection model for early voltage and current	41

	gain	
3.3	CONCLUSION	44
CHAPTER 4:	RESULT AND DISCUSSION	45
4.1	INTRODUCTION	45
4.2	RESULT AND DISCUSSIONS	45
	4.2.1 Distribution of minority carrier within the base ($n_{ieInGaAs}$)	46
	4.2.2 Electric field profile	53
	4.2.3 Diffusivity profile	57
	4.2.4 Early voltage profile	70
	4.2.5 Collector current density (J_{CO}) and common emitter current gain (β)	65
4.3	CONCLUSION	70
CHAPTER 5:	CONCLUSION	71
5.1	CONCLUSION	71
5.2	SUGGESTIONS FOR FUTURE WORK	71
REFERENCES		73
APPENDIX		78

LIST OF TABLES

Name	Caption	Page
Table 1.1	Different type of transistors (adapted from [21])	6
Table 1.1	Some common materials used for HBT(reproduced from [26])	14
Table 4.1	Calculated value showing current gain and Early voltage for various y_C and y_E combination	70

LIST OF FIGURES

Name	Caption	Page
Fig 1.1	Microphotograph of a cutaway model of a transistor	3
Fig 1.2	Experimental transistor (1953)	4
Fig 1.3	Transistor and Integrated Circuits (ICs) chronology [Source: Bell Labs].	5
Fig 1.4	Schematic symbols for PNP- and NPN-type BJTs.	7
Fig 1.5	The schematic diagram of an n^+p-n bipolar junction transistor. Conventional direction of current flow is assumed	10
Fig 1.6	NPN transistor connection	10
Fig 1.7	(a) Flat band diagram of an HBT (b) Energy band diagram under forward active bias	13
Fig 1.8	The three types of semiconductor heterojunctions organized by band alignment.	16
Fig 1.9	Energy gap versus gallium composition for <i>InGaAs</i>	17
Fig 1.10	<i>InGaAs/GaAs</i> HBT (a) with superlattice-base structure (b) without superlattice-base structure	18
Fig 1.11	The schematic diagram showing the cross section of a <i>InGaAs</i> heterojunction bipolar transistor.	19
Fig 2.1	Variation of the minority-carrier distribution in the base quasi-neutral region due to a variation of the base-collector voltage	23
Fig 2.2	Collector current increase with an increase of the collector-emitter voltage due to the Early effect.	24
Fig 2.3	The neutral (i.e. active) base is green, and the depleted base regions are hashed light green. The neutral emitter and collector regions are dark blue and the depleted regions hashed light blue. Under increased collector–base reverse bias, the lower panel of Figure 1 shows a widening of the depletion region in the base and the associated narrowing of the neutral base region.	25

Fig 3.1	Indium mole fraction distribution within the base of a $In_{1-x}Ga_xAs$ HBT for various geometric profiles	36
Fig 3.2	One-dimensional view of an $n-p-n$ $In_{1-x}Ga_xAs$ heterojunction bipolar transistor showing flow of injected minority carrier and current density	37
Fig 4.1a	Effective intrinsic carrier concentration ($n_{ieInGaAs}$) throughout the base region for uniform base doping profile for two value of y_C (0.01 and 0.5) and single value of y_E (0.01).	47
Fig 4.1b	Effective intrinsic carrier concentration ($n_{ieInGaAs}$) throughout the base region for exponential base doping profile for two value of y_C (0.01 and 0.5) and single value of y_E (0.01)	48
Fig 4.1c	Effective intrinsic carrier concentration ($n_{ieInGaAs}$) throughout the base region for uniform and exponential base doping profiles for two value of y_C (0.01 and 0.5) and single value of y_E (0.01).	49
Fig 4.2a	Intrinsic carrier concentration at base-emitter junction($x=0$) and base-collector junction ($x=W_B$) for varying y_C at uniform base doping profile.	50
Fig 4.2b	Intrinsic carrier concentration at base-emitter junction($x=0$) and base-collector junction ($x=W_B$) for varying y_C at exponential base doping profile	51
Fig 4.2c	Intrinsic carrier concentration at base-emitter junction($x=0$) and base-collector junction ($x=W_B$) for varying y_C uniform and exponential base doping profile.	52
Fig 4.3a	Electric field at base-collector junction $E_{InGaAs}(W_B)$ (Red line) and base-emitter junction $E_{InGaAs}(0)$ (black line)for $y_E=.01$ and varying y_C (0.01 ~ 0.5) for uniform doping profile	54
Fig 4.3b	Electric field at base-collector junction $E_{InGaAs}(W_B)$ (Red line) and base-emitter junction $E_{InGaAs}(0)$ (black line) for $y_E=.01$ and varying y_C (.01 ~ .5) for exponential doping profile	55

Fig 4.3c	Electric field at base-collector junction $E_{InGaAs}(W_B)$ (Red line and pink line) and base-emitter junction $E_{InGaAs}(0)$ (black line and blue line) for $y_E=.01$ and varying y_C (.01 ~ 0.5) for uniform and exponential profiles	56
Fig 4.4a	Diffusion coefficient at base-collector junction $D_{nInGaAs}(W_B)$ considering velocity saturation for $y_E=.01, y_C=.5$ and varying base doping $N_B(0)$ for uniform base doping profile.	57
Fig 4.4b	Diffusion coefficient at base-collector junction $D_{nInGaAs}(W_B)$ considering velocity saturation for $y_E=0.01, y_C=0.5$ and varying base doping $N_B(0)$ for exponential base doping profile.	58
Fig 4.4c	Diffusion coefficient at base-collector junction $D_{nInGaAs}(W_B)$ considering velocity saturation for $y_E =0.01, y_C =0.5$ and varying base doping $N_B(0)$ for both uniform and exponential base doping profile	59
Fig 4.5a	Early voltage for $y_E=.01$ and varying y_C for uniform base doping profile. Base width W_B is 500\AA , base doping is 10^{19} cm^{-3}	60
Fig 4.5b	Early voltage for $y_E=.01$ and varying y_C for exponential base doping profile. Base width W_B is 500\AA , peak doping at base-emitter junction is 10^{19} cm^{-3} and minimum doping at base-collector junction is 10^{17} cm^{-3} .	61
Fig 4.5c	Early voltages for $y_E=.01$ and varying y_C for uniform and exponential base doping profiles. Base width W_B is 500\AA , peak doping at base-emitter junction is 10^{19} cm^{-3} and minimum doping at base-collector junction is 10^{17} cm^{-3} for exponential base profile and base doping is considered 10^{19} cm^{-3} for uniform base profile.	62
Fig 4.6	Early voltage for $y_C=0.5$ and varying y_E for exponential and uniform base doping profiles. Base width, W_B is 500\AA , peak doping at base-emitter junction is 10^{19} cm^{-3} and minimum doping at base-collector junction is 10^{17} cm^{-3} .	63
Fig 4.7a	Early voltage (V_A) for triangular indium profile with $y_C=0.5$ and $y_E=0.01$ with varying base doping. Doping concentration at base-collector junction for uniform doping $N_B(W_B) = N_B(0)$ and for exponential doped $N_B(W_B) = N_B(0)/100$	64

Fig 4.7b	Early voltage (V_A) for exponential doping profile with the variation of m_{exp} .	65
Fig 4.8a	Collector saturation current density (J_{CO}) for fixed y_E (0.01) and varying y_C for uniform base doping profile	66
Fig 4.8b	Collector saturation current density (J_{CO}) for fixed y_E (0.01) and varying y_C for uniform base doping profile.	67
Fig 4.8c	Collector saturation current density (J_{CO}) for fixed y_E (0.01) and varying y_C for uniform and exponential base doping profile	68
Fig 4.9	Common emitter current gain (β) for $y_E=0.2$ and varying y_C for uniform and exponential base doping. J_{BO} is considered 7 pA/cm^2 .	69

LIST OF ABBREVIATIONS

<u>ABBREVIATION</u>	<u>ELABORATION</u>
CB	Conduction Band
BC	Base-collector
DHBT	Double Heterojunction Bipolar Transistor
e.g.	For example
MOSFET	Metal-Oxide-Semiconductor Field-Effect Transistor
IGBT	Insulated Gate Bipolar Transistor
IC	Integrated Circuit
JFET	Junction Field Effect Transistor
op-amps	Operational amplifier
MBE	Molecular Beam Epitaxy
MOS	Metal Oxide Semiconductor
EB	Emitter-Base
ECL	Emitter Coupled Logic
HFET	Heterojunction Field Effect Transistor
HEMT	High Electron Mobility Transistor
HBT	Heterojunction Bipolar Transistor
GHz	Giga Hertz
FET	Field Effect Transistor
etc	et cetera

ABBREVIATION **ELABORATION**

SHBT	Single Heterojunction Bipolar Transistor
VB	Valance Band
VCO	Voltage Controlled Oscillators
DOS.	Density of States
CVD	Chemical Vapour Deposition
vs	versus

LIST OF SYMBOLS

<u>SYMBOL</u>	<u>DESCRIPTION</u>
I_B	Base current
I_C	Collector current
I_E	Emitter current
β	Current gain
f	Frequency
f_r	Unity gain cut off frequency
f_{max}	Maximum oscillation frequency
GaAs	Gallium Arsenide
In	Indium
InGaAs	Indium Gallium Arsenide
J_p	Current density for holes
J_n	Current density for electron
J_{nl}	Electron current density for low injection region
J_c	Collector current density
y_{av}	Average In mole fraction
a	0.7743
b	$1+3y_{av}$
c	$0.342/[0.342+ y_{av} (1- y_{av})]$
x	Distance along base
y	In mole fraction
y_c	In fraction at the collector end of the base
y_E	Indium fraction at emitter end of the base
y_D	In dose
γ_E	Emitter charge storage delay time
γ_C	Total delay time from emitter collector
v_s	Saturation velocity in GaAs
v_{sA}	Saturation velocity in InGaAs alloy

<u>SYMBOL</u>	<u>DESCRIPTION</u>
$D_n(x)$	Diffusion co-efficient of electron
D_{max}	Maximum value of diffusion co-efficient
D_n	Diffusion co-efficient of electron EB junction
D_{no}	103.6 cm ² /s
$D_p(x)$	Diffusion co-efficient of hole
$D_{nInGaAs}$	Diffusion co-efficient of electron at InGaAs alloy
$n_{ie}(x)$	Effective intrinsic carrier concentration
$n_{ieGaAs}(x)$	Effective intrinsic carrier concentration for GaAs
$n_{ieInGaAs}$	Effective intrinsic carrier concentration for InGaAs
$n(x)$	Injected minority carrier for all level of injection
$n_l(x)$	Injected minority carrier for low injection
$n(0)$	Injected electron concentration at EB junction for all injection
$N_B(x)$	Base doping concentration
$N_B(0)$	Peak base doping concentration
N_r	Reference concentration
$p(x)$	Hole concentration in the base
$\mu_n(x)$	Electron mobility
$\mu_p(x)$	Hole mobility
$\mu_{nInGaAs}(x)$	Electron mobility inside InGaAs alloy
$E(x)$	Electric field
E_c	Critical electric field
E_{InGaAs}	Electric field inside InGaAs alloy under low injection
E_{InGaAs}	Electric field inside InGaAs alloy under all level of injection
W_B	Basw width
W_{BC}	Width for base collector space charge layer
E_g	Energy gap between conduction and valance band
$D_{EgIn}(x)$	Bandgap narrowing due to the pressure of Ge
$D_{EgHD}(x)$	Bandgap narrowing due to heavy doping
D_{ECG}	Difference between conduction band energies

<u>SYMBOL</u>	<u>DESCRIPTION</u>
γ	1~2
γ_1	0.42
γ_2	$V_{gHD}/V_T = 0.69$
γ_3	V_{gGe}/V_T
γ_r	Ratio of effective DOS in InGaAs to the effective DOS in GaAs
V_{gIn}	750mV
V_{gHD}	18mV
V_T	Thermal voltage
V_A	Early voltage
η	Slope of base doping
η_{In}	Gradient of In mole fraction
C_{EB}	Emitter base depletion capacitance
C_{BC}	Base collector depletion capacitance
R_B	Intrinsic base resistance
R_C	Collector resistance
r_o	Stator resistance
m	Ratio of slope of base doping to base width
m_{IN}	Ratio of gradient in In mole fraction to base width
m_1	$M\gamma_1$
m_2	$m\gamma_2$
m_3	$m_{IN}\gamma_3$
m_{32}	$m_3 - m_2$
m_{023}	$m + m_{32}$
m_{012}	$n(1 + \gamma_1 - \gamma_2)/W_B$
m_{0123}	$m_{012} + m_3$
g_m	Trans conductance
K	Boltzmann constant
T	Absolute temperature
InAlAs	Indium Aluminum Arsenide

<u>SYMBOL</u>	<u>DESCRIPTION</u>
InP	Indium Phosphide
SiC	Silicon Carbide
q	Electron charge

ACKNOWLEDGEMENTS

All thanks belongs to Almighty Allah who has created us and helped us to do all deeds on earth, also who has united many kind hearts to accomplish any great job for mankind.

The author like to express their sincere gratitude to the supervisor, Yeasir Arafat, Assistant Professor of EEE Department, BUET for his tremendous efforts by both encouraging and guiding from the very beginning of this thesis to final draft. The author is highly obliged to their supervisor for spending his lots of valuable times, also for close monitoring every step of this work. The author owes him for continuous supervision and valuable advices, without which it might not be possible at all. Besides that he also helped the author with his wholehearted assistance during the period of understanding previous research related to this work and makes a deep insight in each section of this research. The author is indebted to their supervisor for the whole life for his generosity and kind sympathy.

Finally, we sincerely thank to our parents, family, and friends, who provide the advice and financial support. The product of this research paper would not be possible without all of them.

ABSTRACT

Early effect is the variation in the width of the base in a bipolar junction transistor (BJT) due to a variation in the applied base-to-collector voltage, named after its discoverer James M. Early. An increase in the collector-base voltage causes a greater reverse bias across the collector-base junction which increases the collector-base depletion region width, and decreasing the channel width of the base, which is defined as “Early Effect”. The early effect has been studied extensively in conventional bipolar junction transistors (BJTs). In the present work closed form analytical model were derived for Early Voltage (V_A) and common emitter current gain (β) for uniform and exponential base doping profiles with arbitrary Indium (In) profiles heterojunction bipolar transistor (HBT). Field depended mobility ($D_{nInGaAs}$), band gap narrowing (BGN) (due to both heavy doping and presence of Indium content in the base) and electron velocity saturation effects (v_s) were considered in this model. The effects of base doping profiles and Indium profiles on V_A and β are observed in this work. Here it is observed that if Indium mole fraction at emitter and (y_E) is 0.01 and it increases at collector and (y_C) from 0.01 to 0.5 it increases V_A exponentially. It can be found from this analysis that y_C increases due to BGN effect, effective intrinsic carrier concentration ($n_{ieInGaAs}$) increases towards base-collector junction which minimizes “Early Effect” and increases V_A . For a particular y_C and y_E , V_A found highest for uniform base doping profiles. The results shows that V_A is proportional to base doping concentration. Also keeping y_C at 0.5 and if y_E vary from 0.01 to 0.5 it reduces V_A . It was also observed that by keeping y_E at 0.01 if y_C can be increased from 0.01 to 0.5 it reduces collector current density (J_{CO}). It can also be observed that v_s has significant impact on both J_{CO} and $D_{nInGaAs}$ for uniform and exponential base doping profiles. The results obtained by using this analytical model compared with the results available in the previous literature and found in good agreement.

